Aerodynamics, Heat Transfer, and Shape Optimization of Turbine Endwalls

Minking K. Chyu (mc47@andrew.cmu.edu)
Department of Mechanical Engineering
Carnegie Mellon University
Pittsburgh, PA 15213

Tom I-P. Shih (tomshih@egr.msu.edu)
Department of Mechanical Engineering
Michigan State University
East Lansing, MI 48842

Terrence W. Simon (tsimon@me.umn.edu)
Mechanical Engineering Department
University of Minnesota
Minneapolis, MN 55455

Carnegie Mellon University/ Michigan State University Team

Minking K. Chyu	Principal Investigator
Tom I-P. Shih	Principal Investigator
Yu-Liang Lin	Research Associate
Xubin Gu	Research Assistant

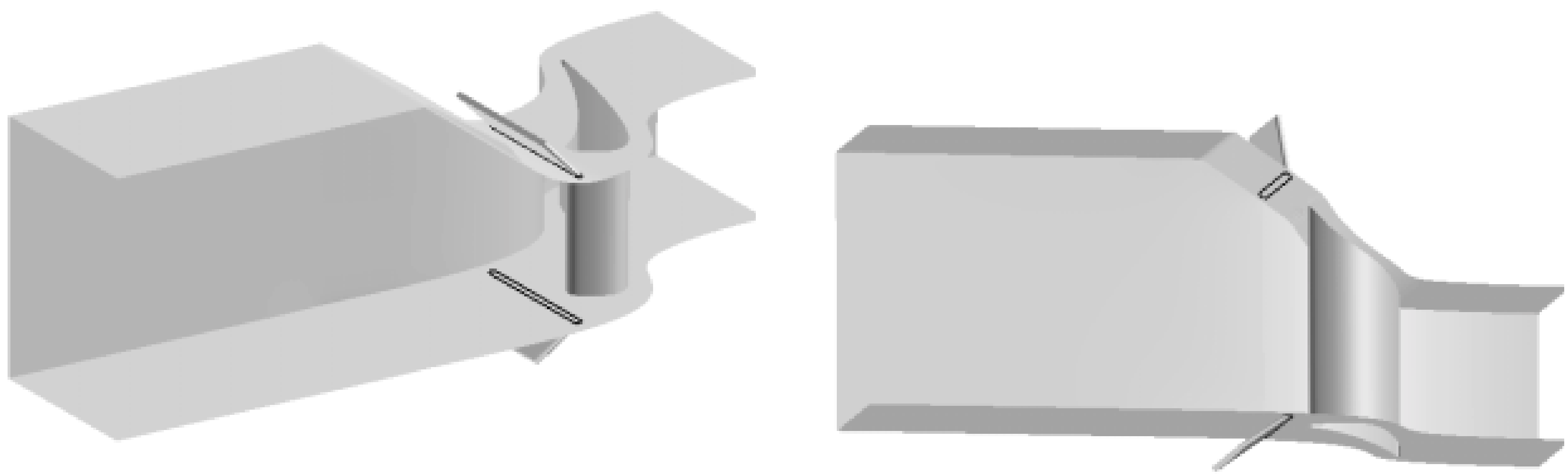

Objectives of CFD Component

Validate/assess CFD code and turbulence models.

Perform CFD simulations to study flow and heat transfer in the combustor-to-stator-transition duct and first-stage stator with and without film cooling.

Develop and optimize design concepts in collaboration with university and industrial partners.

Computational Approach

Governing Equations

continuity
compressible Navier-Stokes
total energy

Turbulence Models

low Reynolds # k-ω
low Reynolds # SST
expl. Algebraic Rey. stress

Algorithm

cell-center finite-volume
density-based
3rd-order flux-difference
diagonalized ADI w/ multigrid
overlapped/patched grids

Code

modified CFL3D
(a research code from
NASA Langley)

Problem Description

Two Locations for the Contouring

(upstream of airfoil only, upstream & through airfoil)

w/ & w/ofilm cooling

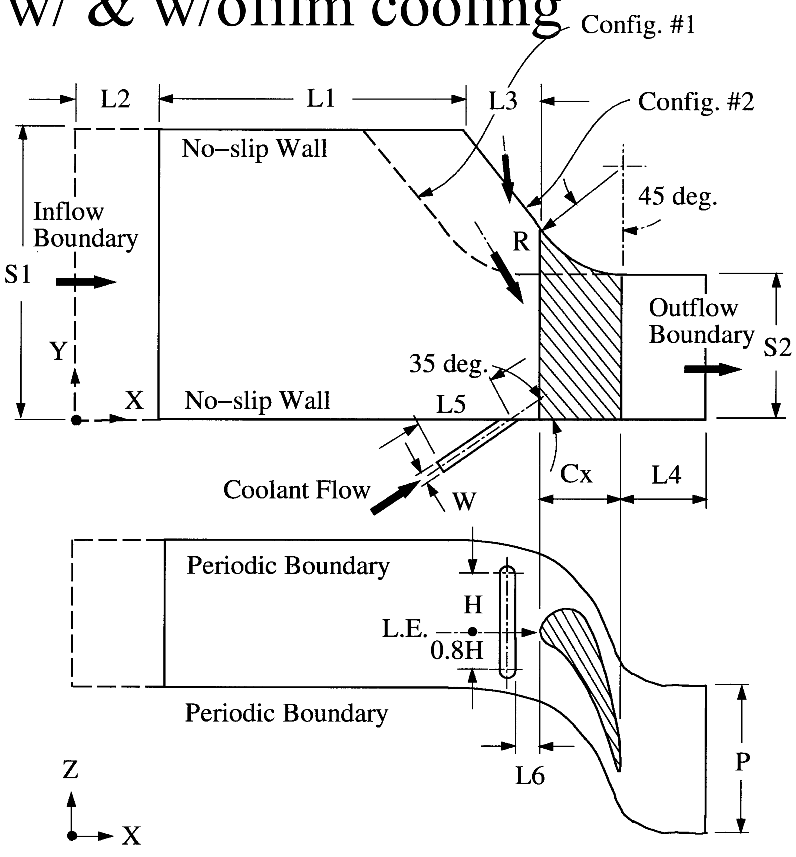

w/ & w/o gap leakage

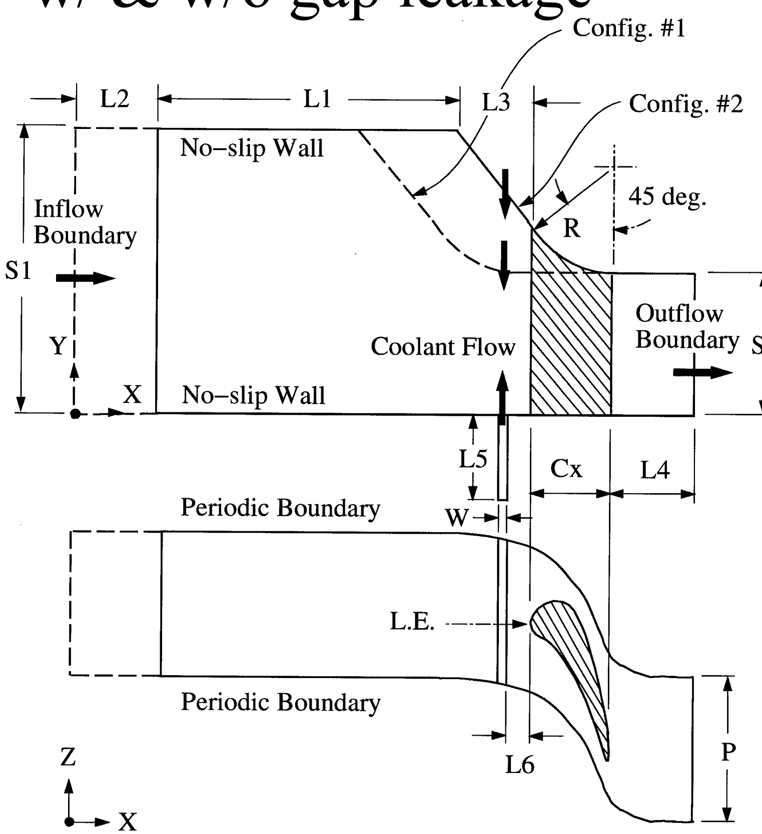

Grid System

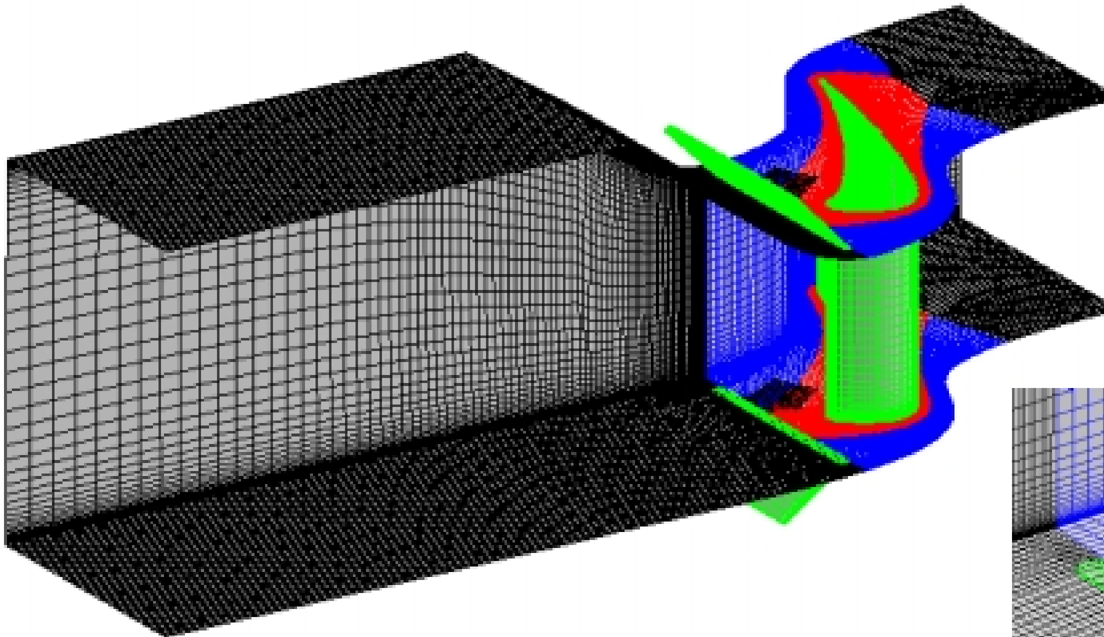

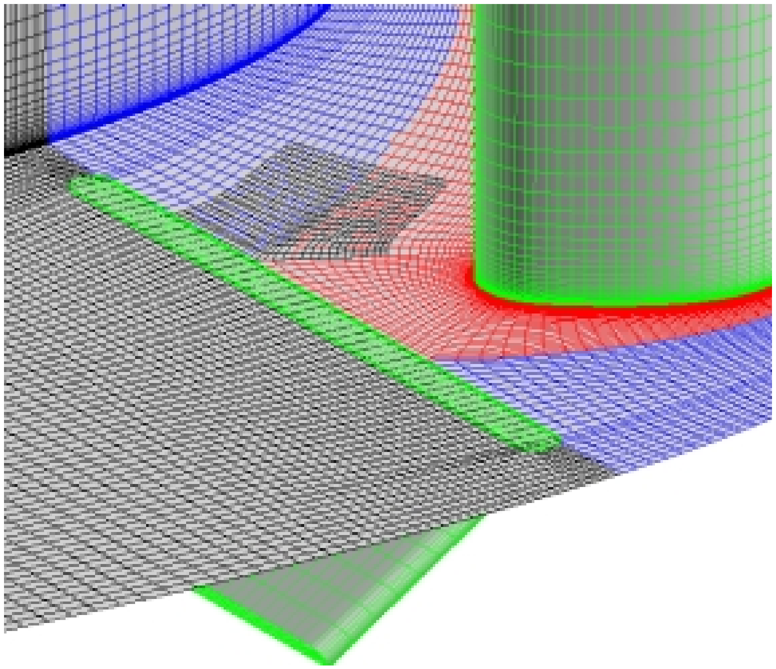

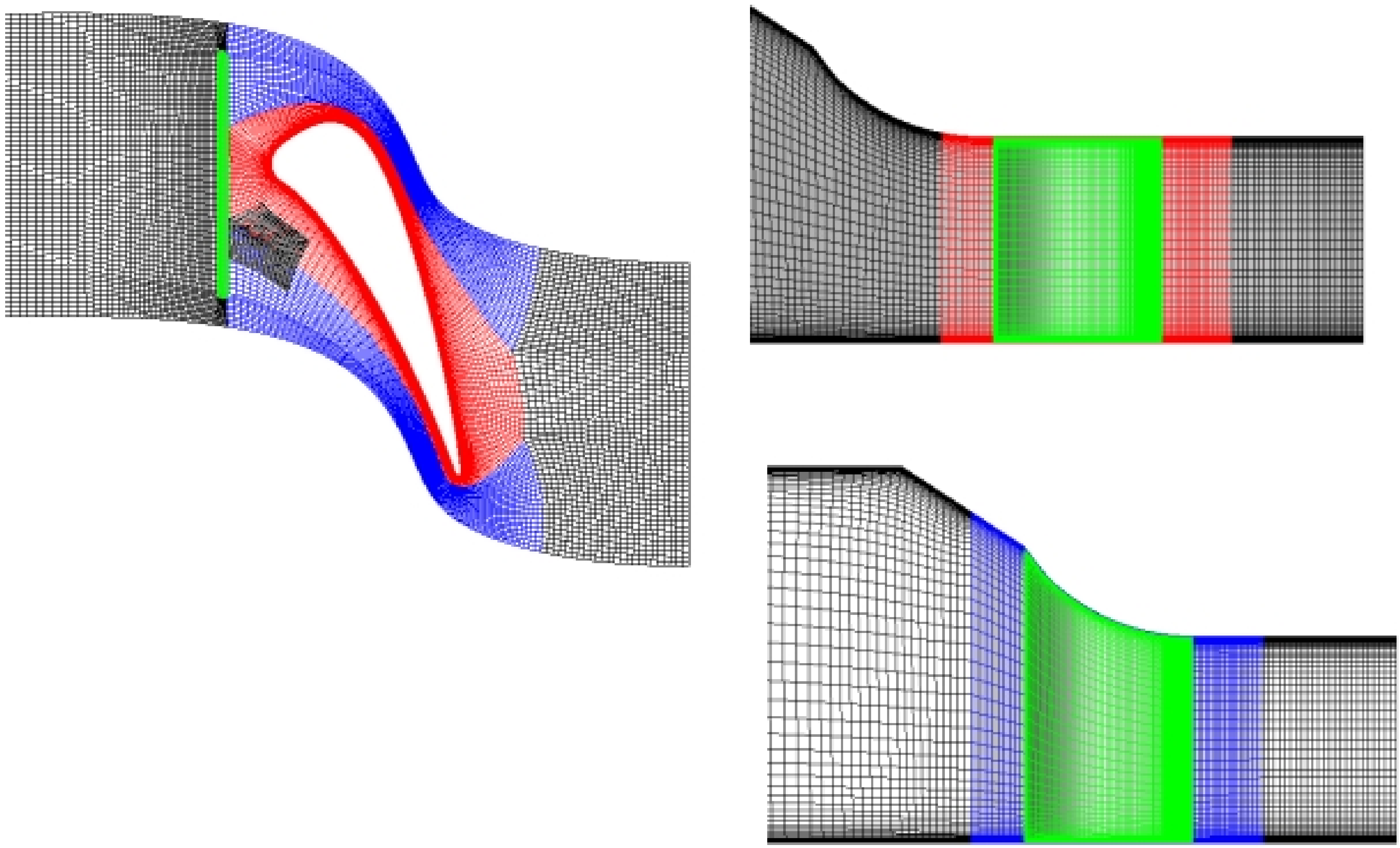

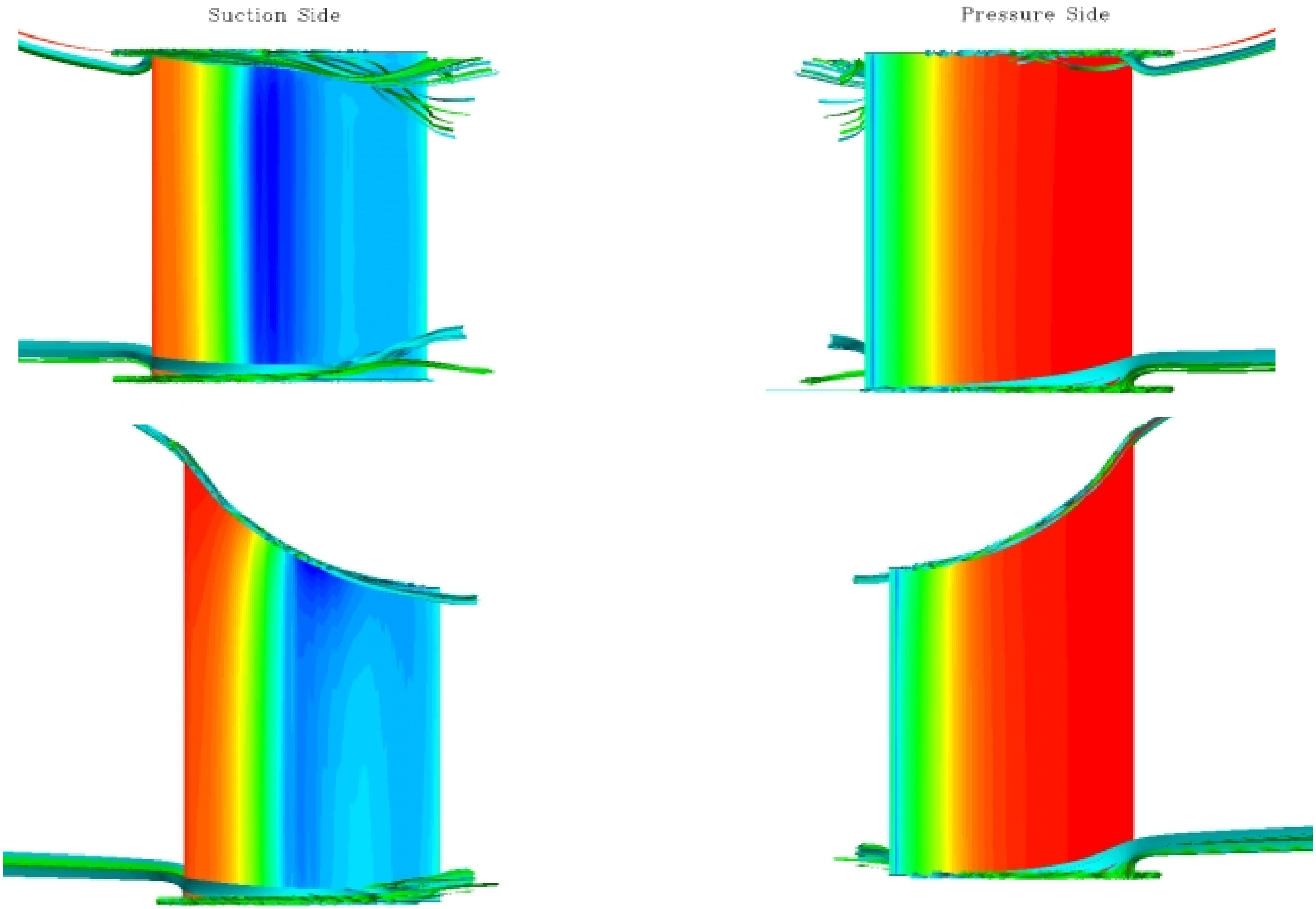
Suction Side
Pressure Side

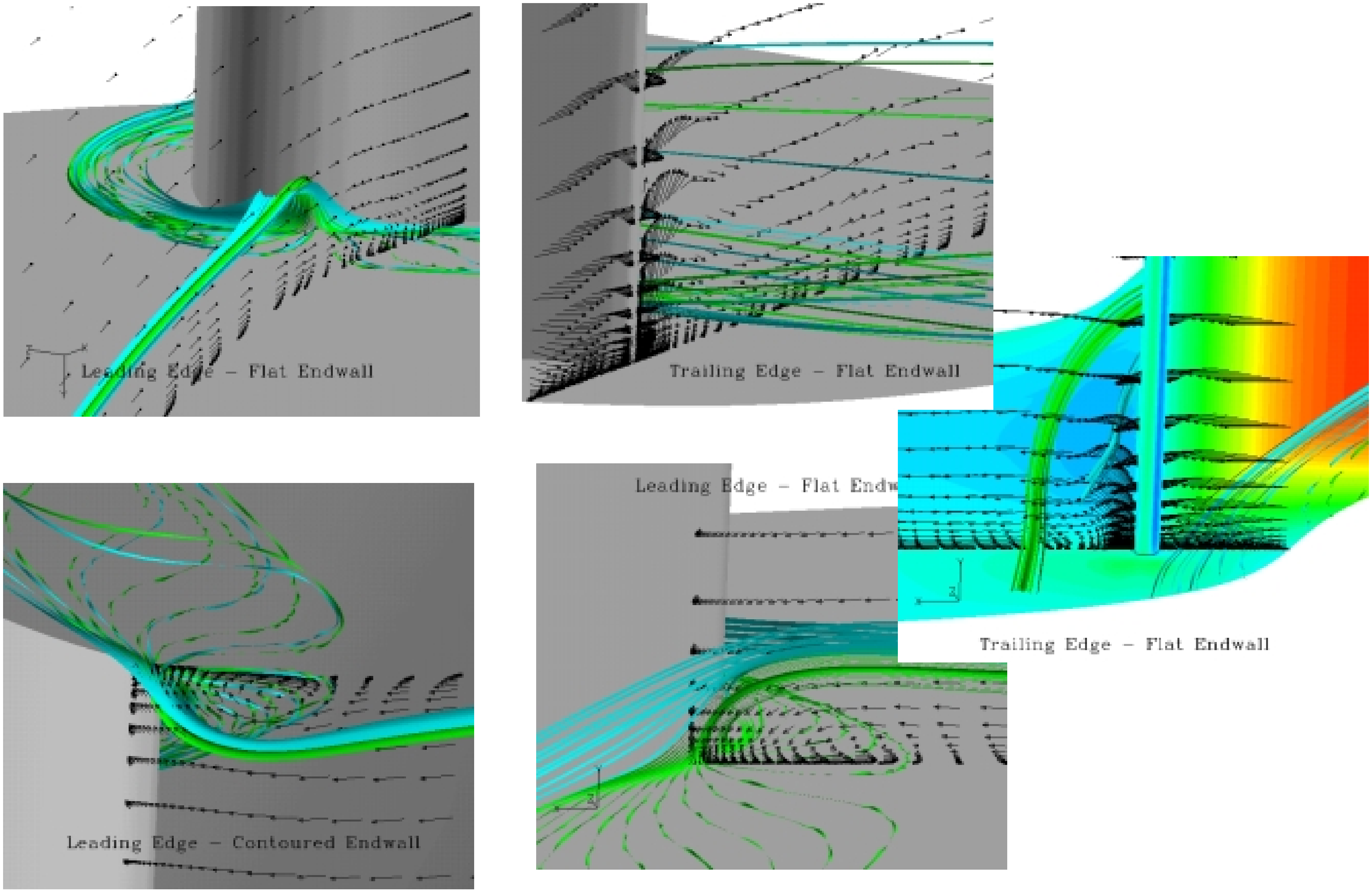
Leading Edge – Flat Endwall
Trailing Edge – Flat Endwall
Leading Edge – Flat Endw
Trailing Edge – Flat Endwall
Leading Edge – Contoured Endwall

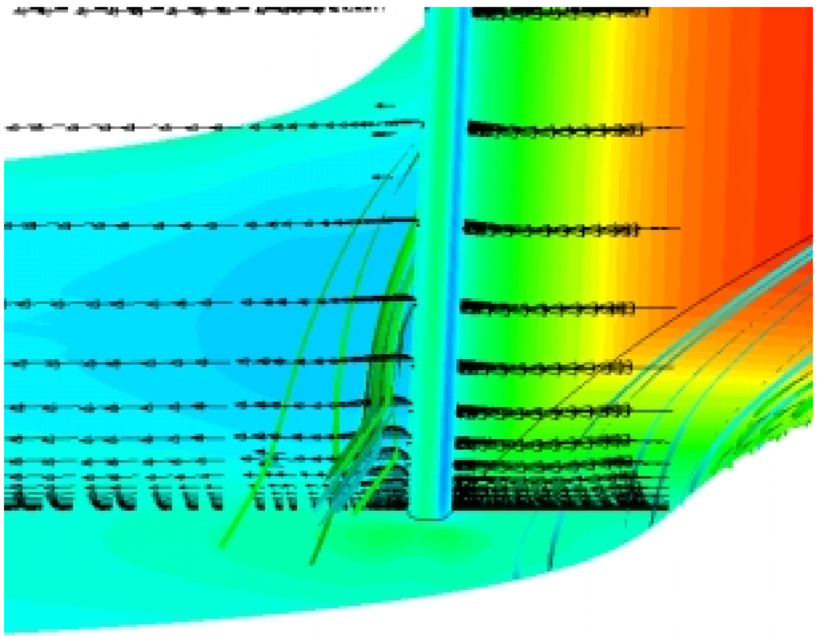

Trailing Edge – Flat Endwall

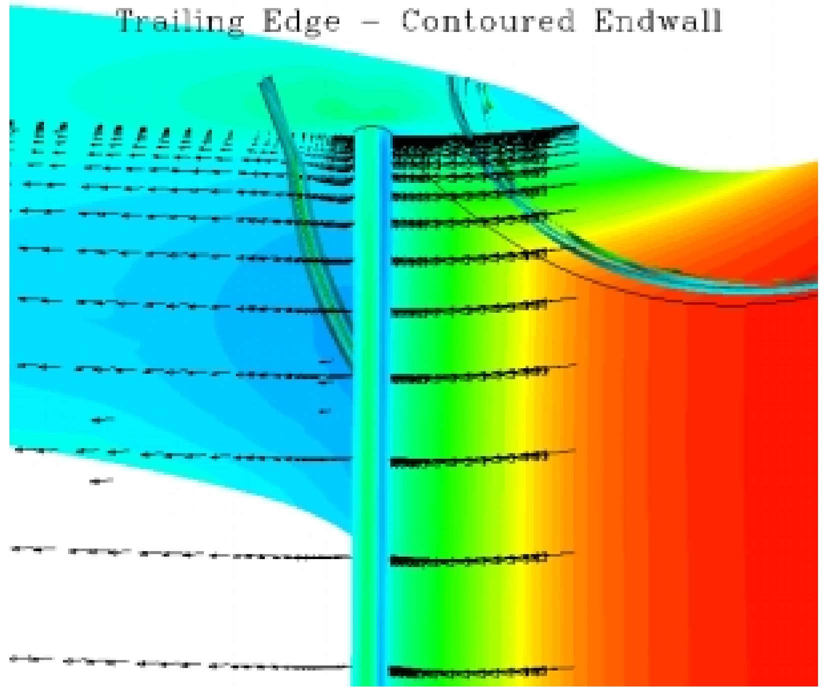

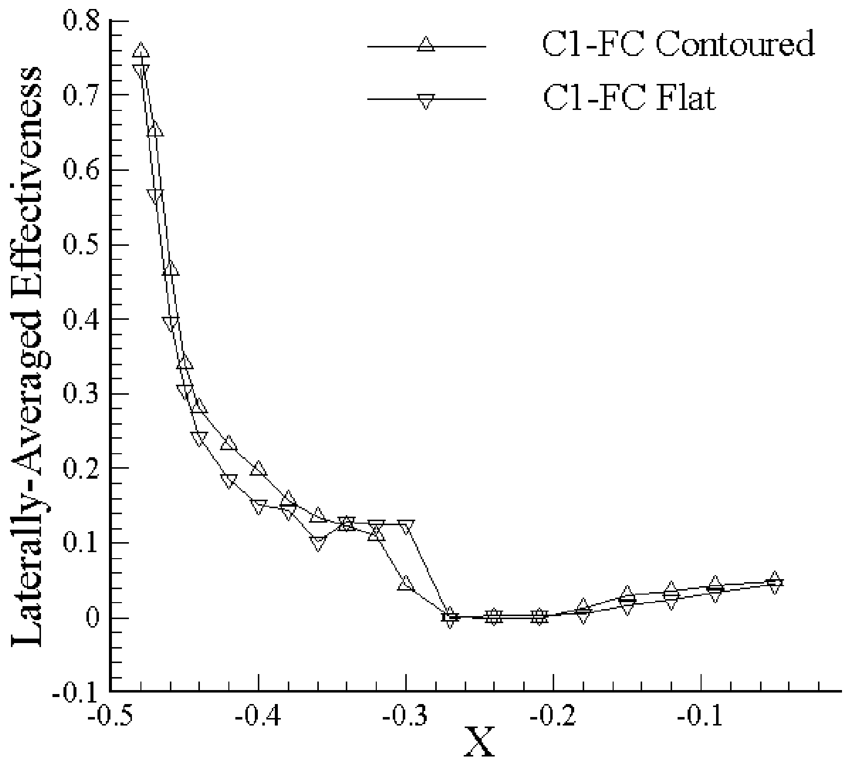

C1-FC Contoured
C1-FC Flat
Laterally-Averaged Effectiveness
X
0.8
0.7
0.6
0.5
0.4
0.3
0.2
0.1
0
-0.1
-0.5
-0.4
-0.3
-0.2
-0.1

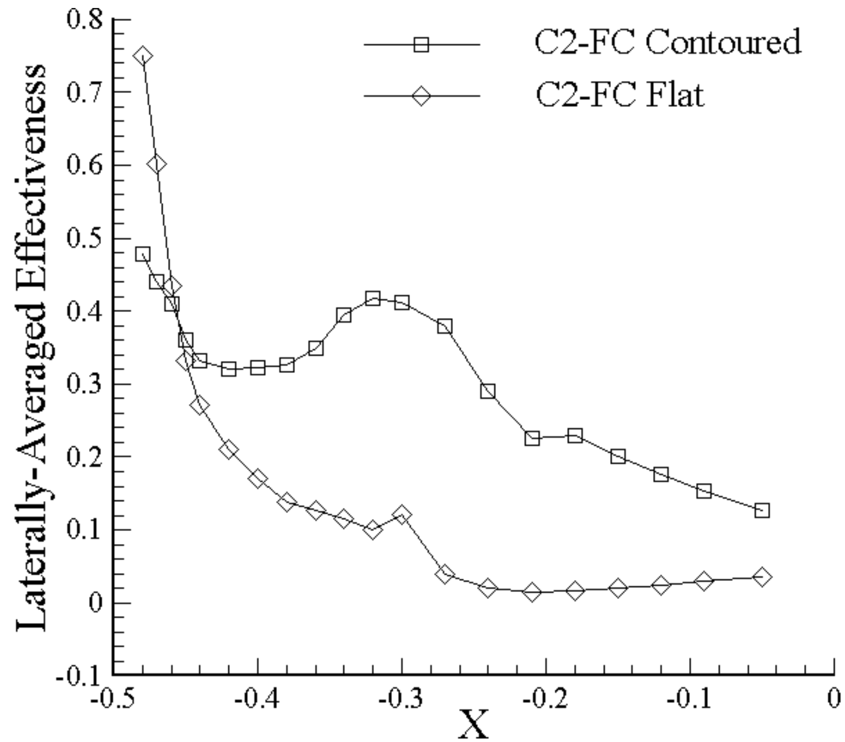

C2-FC Contoured
C2-FC Flat
Laterally-Averaged Effectiveness
X
0.8
0.7
0.6
0.5
0.4
0.3
0.2
0.1
0
-0.1
-0.5
-0.4
-0.3
-0.2
-0.1
0

Conclusions

- When the contouring is all upstream of the airfoil, secondary flows on both the flat and the contoured endwalls were similar in magnitude.

- When the contouring starts upstream of the airfoil and continues through it, secondary flows on the contoured endwall are markedly weaker than those on the flat endwall.

- With less secondary flows on the contoured endwall, film-cooling effectiveness improve considerably there.

UNIVERSITY OF MINNESOTA TEAM

Terry Simon	**Principal Investigator**
Rohit Oke	**Research Assistant**
Steve Burd	**Research Assistant**
Cynthia Satterness	**Research Assistant**

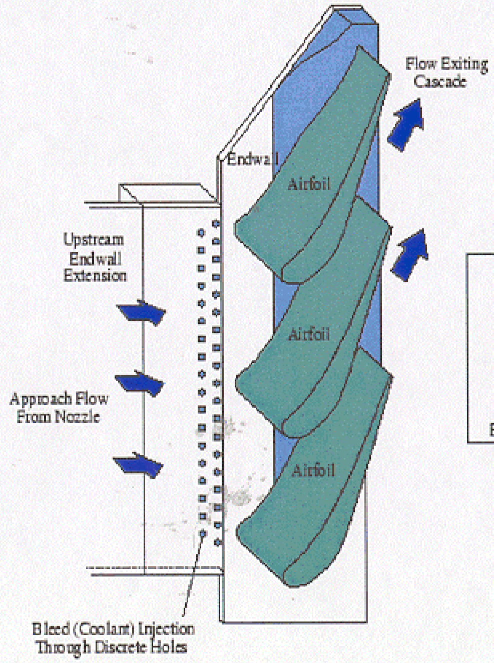

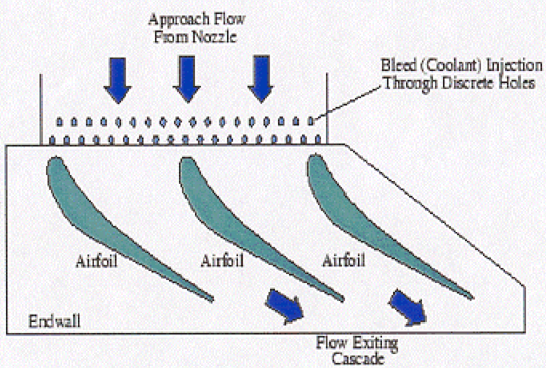

Comparison of Velocities for different BFR's, Discrete Hole Injection , at $x/C_{ax} = 0.90$

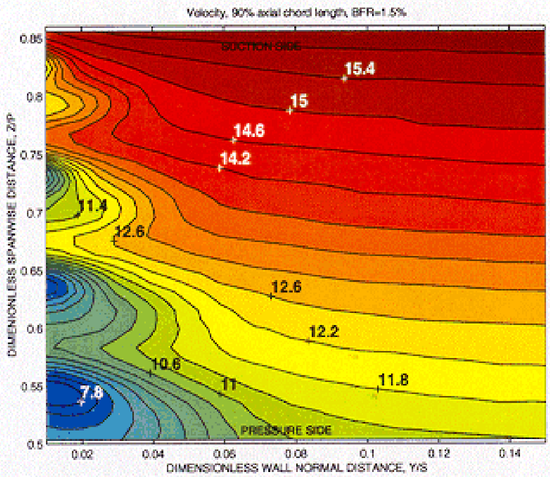

BFR = 1.5 %

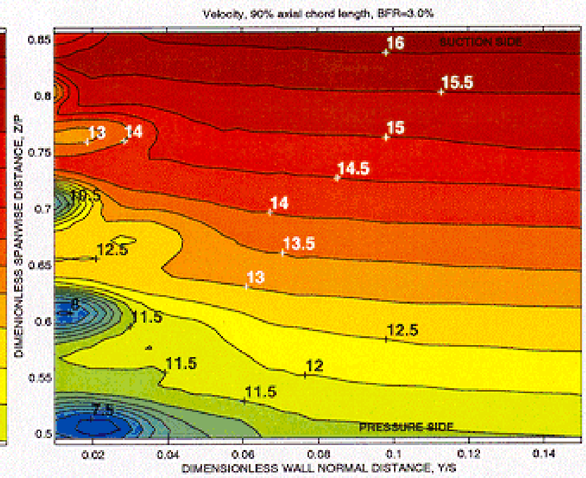

BFR = 3.0%

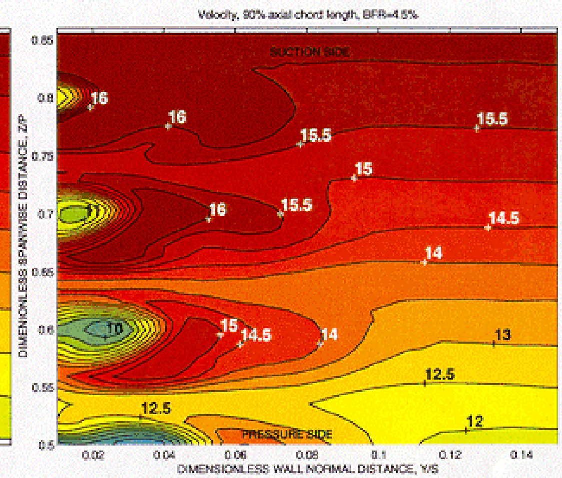

BFR = 4.5%

The following figures compare velocity contours at $x/C_{ax} = 0.9$ for different BFR's. It is seen that the core flow has strong velocity gradients in all the cases. These are due to the gradients in the approach flow velocity as it adjusts to enter the passage. The bleed flow does not have a strong influence on the core flow. Observe the pockets of higher velocity above the cores of the jets with higher blowing ratios. As the blowing ratio increases, bleed flow causes increased blockage and the core flow accelerates around this blockage. Observe that due to passage flow velocity gradients, there is a span variation of injection velocity. This can be significant to designers.

Comparison of Recovery Temperatures for different Streamwise Positions, Discrete Hole Injection , BFR = 3.0 %

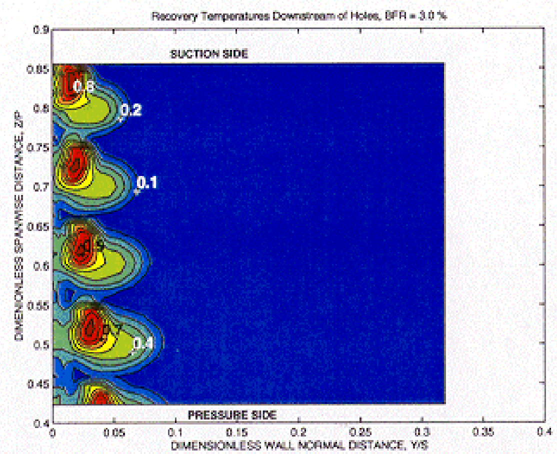

Downstream of Holes, i.e x/C_{ax} = -0.10%

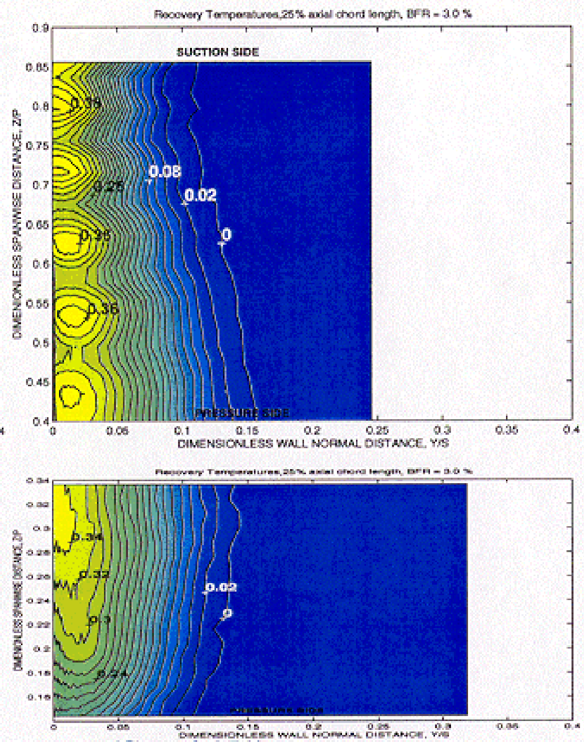

x/C_{ax} = 0.25%

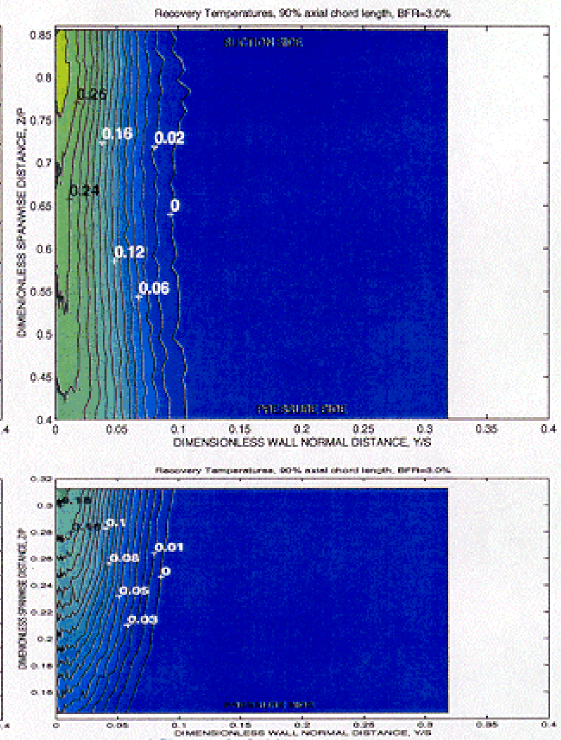

x/C_{ax} = 0.9%

The following figures compare θ contours at different planes for the same BFR. Observe the rapid decay of the θ contours due to the strong mixing with discrete hole jets. By x/C_{ax} = 0.25, adjacent jets close to the suction side have not merged. However, towards the pressure side, adjacent jets have merged. By x/C_{ax} = 0.9 the jets have merged across the span and signs of coolant migration towards the suction side are observed.

Comparison of Recovery Temperatures for Slot Injection with Discrete Hole Injection

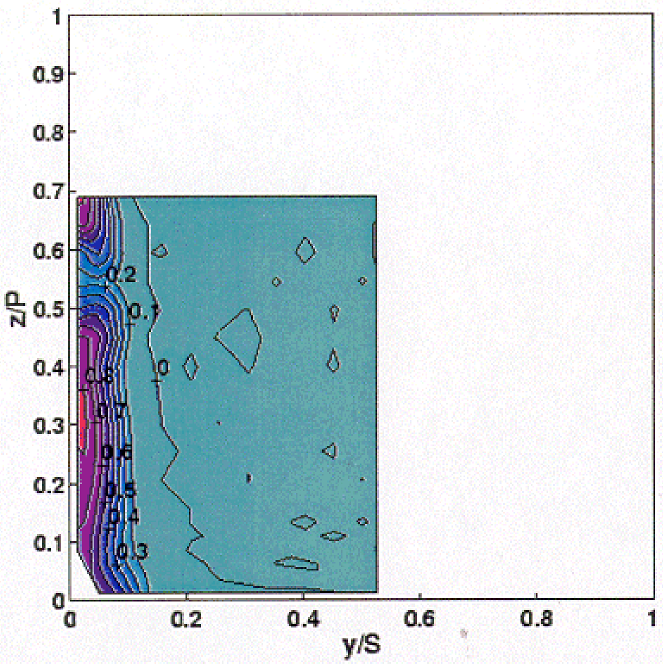

Recovery Temperature, Slot Injection, x/Cax = 0.15, BFR = 3.2 %

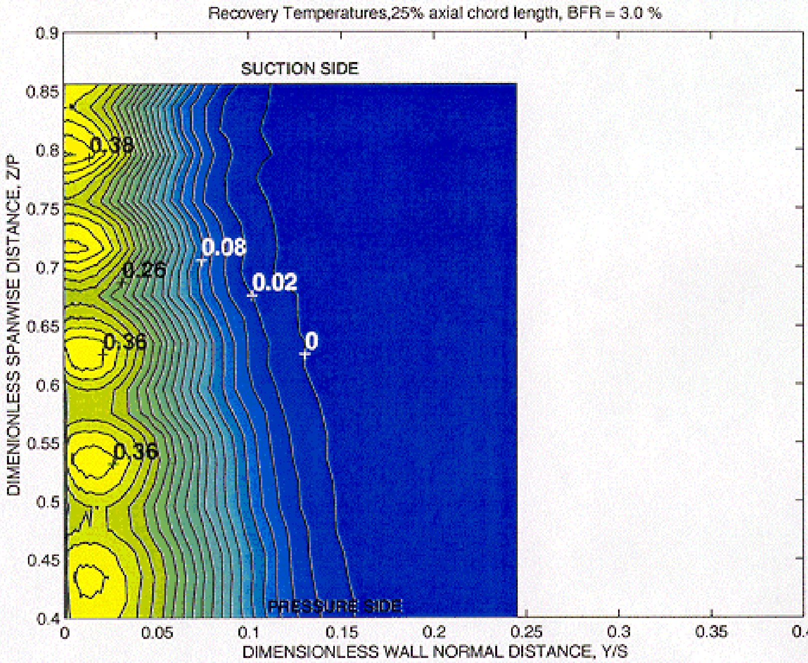

Recovery Temperature, Discrete Hole Injection, x/Cax = 0.25, BFR = 3.0 %

The two figure above show comparisons of θ contours for slot and discrete hole injection. Observe the lower levels of the θ contours for the discrete hole injection case. This is because with the same blowing ratio the discrete hole jets have a higher velocity than that of the slot-injected jets. Thus, mixing with the main stream flow is higher with discrete hole injection. (Note that the color scheme for the two figures do not match)

Comparison of Recovery Temperatures for Different BFR's, Discrete Hole Injection , at $x/C_{ax} = 0.27$

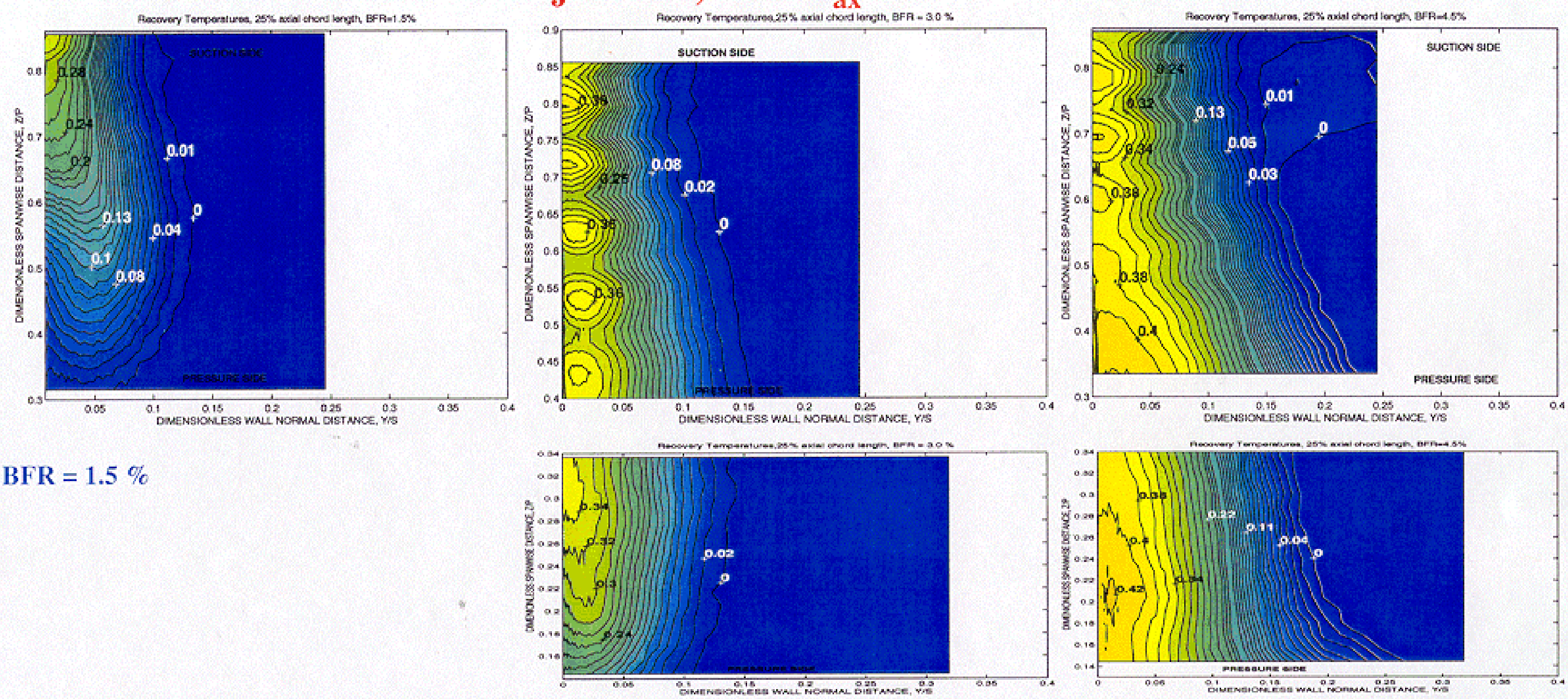

BFR = 1.5 %

BFR = 3.0%

BFR = 4.5%

The above figures compare θ contours for different axial planes with different BFR's. At BFR = 1.5%, blowing is sufficiently low that coolant migrates to the suction surface. For the higher-BFR cases, no migration of the coolant is observed. Note the significantly higher increase in the peak θ value from BFR = 1.5% to BRF=3.0%. The peak values near the suction surface do not rise significantly with further increases in BFR.

Recovery Temperature Distributions for Full Slot Bleed Injection at x/C_{ax} = 0.15, 0.5, 0.9, BFR = 3.2%

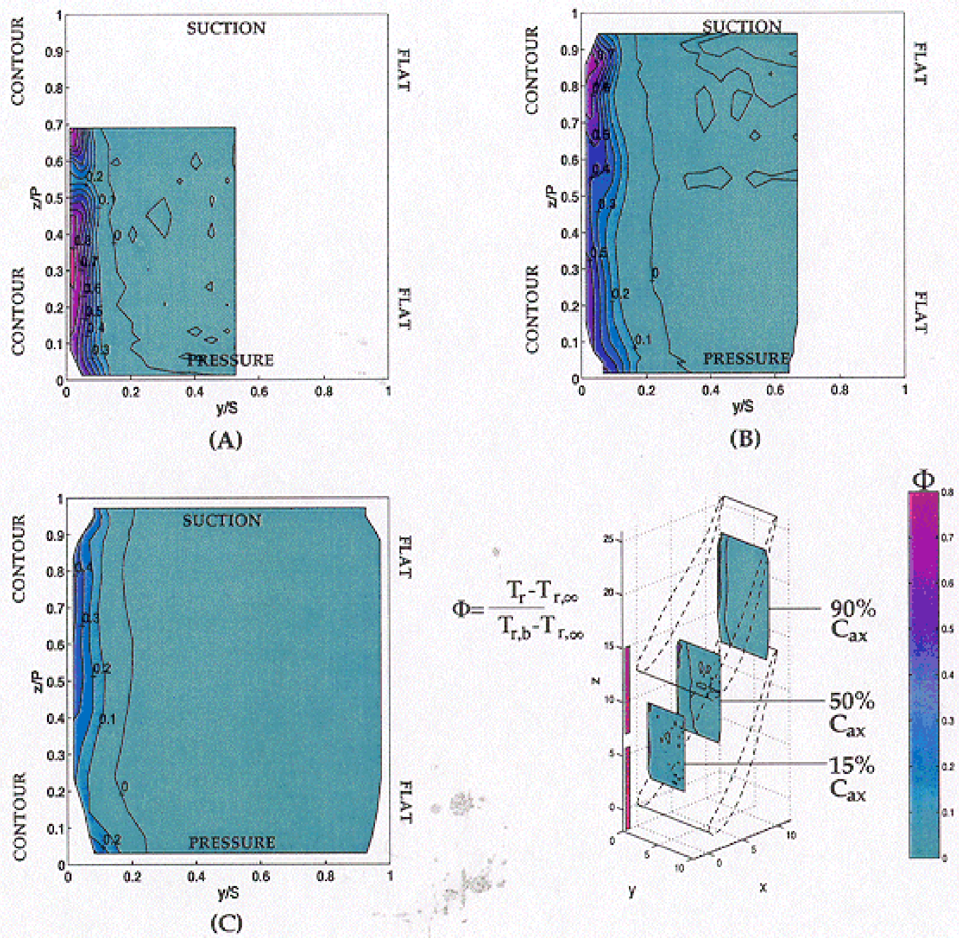

The figures show the streamwise development of the recovery temperature contours. Observe the decay of the θ contours with streamwise position. Note that there is nearly uniform bleed flow coverage along the spanwise direction, with adequate coverage on the suction and pressure side endwall corners. Of the cases studied, this blowing ratio was found to be best in terms of adequate coverage near the endwall corners. If the bleed flow ratio is decreased, coolant tends to migrate to the suction side. Higher bleed flow ratios on the other hand promote coolant migration on the pressure endwall corner.